SYSTEM'S NONLINEARITY MEASUREMENT BASED ON THE RPN CONCEPT

M. Farenzena and J. O. Trierweiler[#]

Group of Integration, Modelling, Simulation, Control and Optimization of Processes (GIMSCOP)
Department of Chemical Engineering, Federal University of Rio Grande do Sul (UFRGS)
Rua Duque de Caxias, 1303 apt. 603 CEP: 90010-283 - Porto Alegre - RS - BRAZIL,
Fax: +55 51 3316 3277, Phone: +55 51 3316 4072
E-MAIL: {farenz, jorge}@enq.ufrgs.br

Abstract: The nRPN, $nRPN_{STAT}$, and $nRPN_{DYN}$ are three novel indexes to measure system's nonlinearity. These nonlinear measurements are derived from the Robust Performance Number (RPN) concept. The total system's nonlinearity can be measured by the *nonlinear RPN* (nRPN), while the purely static nonlinearity is captured by nonlinear static RPN ($nRPN_{STAT}$) and the dynamic component by the nonlinear dynamic RPN ($nRPN_{DYN}$). The novel indexes do not require a nonlinear model, being enough a set of linear models. Therefore, they can easily be applied to quantify the nonlinearities of industrial plants and used to answer several practical important questions such as: How nonlinear is the system? Is it necessary to apply a nonlinear controller? What kind of nonlinear controller is necessary? *Copyright © 2004 IFAC*

Keywords: - nonlinearity, nonlinearity measurements, controller selection, RPN Methodology, benzene distillation column

1 INTRODUCTION

Is a nonlinear controller necessary? If the answer is yes, what kind of nonlinear controller is required? Nowadays, questions like these arise frequently. To answer these questions it is necessary to quantify the process nonlinearity degree. When the degree of nonlinearity is low, a linear controller can be applied without performance loss. Linear controllers are much simpler to tune and to maintain. Therefore, one will invest in a nonlinear controller when is really necessary. Many times, simple nonlinear gain compensation is enough to significantly improve the control performance. In other situations, the process dynamic also changes considerably. In these situations, the nonlinear controller must also compensate the system's dynamic and the nonlinear controller becomes more difficult to tune and to implement. In this work, three novel nonlinear measurements (nRPN, $nRPN_{STAT}$, and $nRPN_{DYN}$) are proposed. These nonlinear measurements are derived from the Robust Performance Number (RPN) concept. The total system's nonlinearity can be measured by the *nonlinear RPN* (nRPN), while the purely static nonlinearity is captured by nonlinear static RPN ($nRPN_{STAT}$) and the dynamic component by the nonlinear dynamic RPN ($nRPN_{DYN}$).

About nonlinear measurements, there is not too much available in the literature. For instance, Guay et al. (1997) proposed a method based on the concavity measure, while Helbig et al. (2000) quantify the degree of nonlinearity based on the best linear approximation to the nonlinear model. These approaches only measure the open-loop degree of nonlinearity and to apply these methodologies it is necessary a nonlinear phenomenological model. Therefore, the practical application is reduced and not so simple.

Trierweiler (1997) and Trierweiler and Engell (1997a) introduced the RPN for a plant set (RPPN) index to quantify the degree of nonlinearity. The

[#] Author to whom the correspondence should be addressed.

RPPN needs only a set of linear models, which can be obtained by identification or linearization of the process in different operating points. The RPPN takes the closed loop performance into account automatically. The novel indices introduced in this paper are improvement of the original RPPN.

This paper is structured as follows: in section 2 a brief description of the RPN methodology will be made. In section 3 the nonlinear RPN will be defined. The nonlinearity degree of a high purity distillation and the quadruple-tank system will be quantified in sections 4 and 5, respectively.

2 THE ROBUST PERFORMANCE NUMBER (RPN)

The RP-number is a measure of how potentially difficult it is for a given system to achieve the desired performance robustly. The RPN of a multivariable plant with transfer matrix $G(s)$ is defined as

$$\mathrm{RPN} \stackrel{\Delta}{=} \Gamma_{\sup}(G,T,\omega) = \sup_{\omega\in\mathrm{R}} \{\Gamma(G,T,\omega)\} \tag{1a}$$

$$\Gamma(G,T,\omega) \stackrel{\Delta}{=} \sqrt{\bar{\sigma}([I-T(j\omega)]T(j\omega))\left(\gamma^*(G(j\omega)) + \frac{1}{\gamma^*(G(j\omega))}\right)} \tag{1b}$$

where $\gamma^*(G(j\omega))$ is the *minimized* condition number of $G(j\omega)$ and $\bar{\sigma}([I-T]T)$ is the maximal singular value of the transfer function $[I\text{-}T]\,T$. T is the attainable desired output complementary sensitivity function that is determined for the nominal model G.

The RPN determined by two factors:

1. $\bar{\sigma}([\mathbf{I}-\mathbf{T}]\mathbf{T})$ This term acts as a weighting function that emphasizes the crossover frequency, that is the most important region for the robust stability, because feedback controller will operate in this region.
2. $\boldsymbol{\gamma^*(G)+1/\gamma^*(G)}$**.** The origin of this term is the analysis of robust performance (RP) of inverse-based controllers (see Trierweiler, 1997).

3 NONLINEAR RPN

The nonlinear RPN (nRPN), nonlinear dynamic RPN ($\mathrm{nRPN_{DYN}}$) and nonlinear static RPN ($\mathrm{nRPN_{STAT}}$) are introduced to measure system's nonlinearity. These nonlinearity measurements are derived from the Robust Performance Number (RPN) concept. The total system's nonlinearity can be measured by the *nonlinear RPN* (nRPN), while the purely static nonlinearity is captured by nonlinear static RPN ($\mathrm{nRPN_{STAT}}$) and the dynamic component by the nonlinear dynamic RPN ($\mathrm{nRPN_{DYN}}$).

3.1 Preliminary definitions

Next, we introduce five concepts, which are used in the definition of nRPN.

***Definition 1*: Minimized condition number of a plant set *P* ($\boldsymbol{\gamma^{\#}(P)}$).** Consider the polytopic system representation P consisting of NP linear models G_i

$$P \in \mathrm{Co}\{G_1,\ldots,G_{NP}\} \stackrel{\Delta}{=} \left\{ \sum_{i=1}^{NP} \alpha_i G_i : \alpha_i \geq 0, \sum_{i=1}^{NP} \alpha_i = 1 \right\}. \tag{2}$$

Then the minimized condition number of P is defined as

$$\begin{aligned} \gamma^{\#}(P) &\stackrel{\Delta}{=} \min_{L^{\#},R^{\#}} \sup \gamma\left(L^{\#} P R^{\#}\right) \\ &= \min_{L^{\#},R^{\#}} \sup\left\{\gamma_1\left(L^{\#} G_1 R^{\#}\right),\ldots,\gamma_{NP}\left(L^{\#} G_{NP} R^{\#}\right)\right\} \end{aligned} \tag{3}$$

where $L^{\#}$ and $R^{\#}$ are the real, diagonal, and nonsingular scaling matrices used to determine $\gamma^{\#}(P)$.

The scaling matrices $L^{\#}$ and $R^{\#}$ can be calculated by the solution of a generalized eigenvalue problem (Trierweiler, 1997).

***Definition 2*: Maximal difference of the minimized condition number for a plant set *P* ($\boldsymbol{\Delta\gamma^{\#}(P)}$)**. For the polytopic model P, the maximal difference in the condition number ($\Delta\gamma^{\#}$(P)) is defined by

$$\begin{aligned} \Delta\gamma^{\#}(P) = \max&\left(\gamma\left(L^{\#} G_1 R^{\#}\right),\ldots,\gamma\left(L^{\#} G_{NP} R^{\#}\right)\right) \\ &- \min\left(\gamma\left(L^{\#} G_1 R^{\#}\right),\ldots,\gamma\left(L^{\#} G_{NP} R^{\#}\right)\right). \end{aligned} \tag{4}$$

***Definition 3*: Maximal singular value ratio of a plant set *P* ($\boldsymbol{\sigma^{\#}(P)}$).** For the polytopic model P, given by (2), the maximal singular value ratio of P is defined by

$$\sigma^{\#}(P(j\omega)) \stackrel{\Delta}{=} \frac{\max\left\{\bar{\sigma}\left(L^{\#} G_1 R^{\#}\right),\ldots,\bar{\sigma}\left(L^{\#} G_{NP} R^{\#}\right)\right\}}{\min\left\{\bar{\sigma}\left(L^{\#} G_1 R^{\#}\right),\ldots,\bar{\sigma}\left(L^{\#} G_{NP} R^{\#}\right)\right\}} \tag{5}$$

where $\bar{\sigma}(L^{\#} G_t R^{\#})$ is the maximal singular value of the scaled model G_i using the scaling matrices $L^{\#}$ and $R^{\#}$.

***Definition 4:* Projection Matrix ($\boldsymbol{M^{\#}(P)}$).** For the polytopic model P, the projection matrix $M^{\#}$ is a symmetric matrix with the elements $m^{\#}_{ij}$ given by

$$m^{\#}_{i,j}(P(0)) \stackrel{\Delta}{=} \max_{k=1..NS}\left[abs\left(u^H_{k,i}\cdot u_{k,j}-1\right), abs\left(v^H_{k,i}\cdot v_{k,j}-1\right)\right] \tag{6}$$

where the vectors $u_{k,i}$ and $v_{k,i}$ are the k^{th} column vectors of the unitary matrices U_i and V_i

$$\begin{aligned} U_i &= \left[\bar{u}_i = u_{1,i}, u_{2,i}, \ldots, u_{no,i} = \underline{u}_i\right] \text{ and} \\ V_i &= \left[\bar{v}_i = v_{1,i}, v_{2,i}, \ldots, v_{ni,i} = \underline{v}_i\right] \end{aligned} \tag{7}$$

obtained by the Singular Value Decomposition (SVD) of the scaled gain matrix of the model i, i.e.,

$$\begin{aligned} L^{\#} G_i(0) R^{\#} &= U_i \Sigma_i V_i^H \\ &= \sum_{k=1}^{NS} \sigma_k\left(L^{\#} G_i(0) R^{\#}\right) u_{k,i} v^H_{k,i} \end{aligned} \tag{8}$$

and Σ_i contains a diagonal nonnegative definite

matrix Σ_{NS} of singular values arranged in descending order:

$$\Sigma = \begin{pmatrix} \Sigma_{NS} \\ 0 \end{pmatrix} \text{ if } no \geq ni \text{ or } \Sigma = \begin{pmatrix} \Sigma_{NS} & 0 \end{pmatrix} \text{ if } no < ni \quad (9)$$

$$\text{and } \Sigma_{NS} = diag(\sigma_1, \sigma_2, ..., \sigma_{NS}),\ NS = \min\{no, ni\} \quad (10)$$

$$\text{with} \qquad \overline{\sigma} = \sigma_1 \geq \sigma_2 \geq ... \geq \sigma_{NS} = \underline{\sigma}\,. \quad (11)$$

***Definition 5*: Projection Factor ($\upsilon^{\#}(P)$).** For the polytopic model P, the projection factor is equal to 10 powered by the greatest element of the projection matrix $M^{\#}$ defined in (13), i.e.,

$$\upsilon^{\#}(P(0)) \stackrel{\Delta}{=} 10\text{^}\max\left(M^{\#}(P(0))\right). \quad (12)$$

The projection factor $\upsilon^{\#}(P)$ is used to detect a change of multivariable gain sign, what is captured by the projection matrix $M^{\#}$.

3.2 Nonlinear RPN curves

Based on $\Delta\gamma^{\#}(P)$, $\sigma^{\#}(P)$, and $\upsilon^{\#}(P)$ we can finally define the nonlinear RPN curves. Here, the nonlinear RPN (nRPN), the nonlinear *static* RPN ($nRPN_{STAT}$), and the nonlinear *dynamic* RPN ($nRPN_{DYN}$) curves are shown. The nRPN curve is used to capture the total process nonlinearity, while $nRPN_{STAT}$ and $nRPN_{DYN}$ are applied to quantify the static and dynamic contributions, respectively.

***Definition 6*: Nonlinear Robust Performance Number curve (nRPN curve, $\Gamma^{\#}$).** The nonlinear RPN curve is defined as

$$\Gamma^{\#}(P,T,\omega) \stackrel{\Delta}{=} \left[\sigma^{\#}(P(j\omega)) + \Delta\gamma^{\#}(P(j\omega))\right]\upsilon^{\#}(P(0))\Gamma(G,T,\omega) \quad (13)$$

where $\Gamma(G,T,\omega)$ is given by (1b). ■

The potential increase of system's directionality is captured by the term ($\Delta\gamma^{\#}(P)$), the modification of the maximal singular value is considered by $\sigma^{\#}(P)$, and the change of the multivariable sign by $\upsilon^{\#}(P)$. From the definition, the nRPN curve is always above the RPN curve.

The nominal model G used in (13) is usually the nominal operating point of the plant, where the process will mostly work. When this operating point cannot be selected among the possible plant models, then the linear model with the worst possible performance should be set as nominal model, i.e., the model with the largest RPN.

The nRPN curve is influenced by static and dynamic nonlinearities. To separate the contribution of each kind of nonlinearity, the $nRPN_{STAT}$ ($\Gamma^{\#}_{STAT}$) and $nRPN_{DYN}$ ($\Gamma^{\#}_{DYN}$) curves are defined, as follows:

$$\Gamma^{\#}_{STAT}(P,T,\omega) \stackrel{\Delta}{=} \Gamma(G,T,\omega) + \min\left(\Gamma^{\#}(P,T,\omega) - \Gamma(G,T,\omega)\right) \quad (14)$$

$$\Gamma^{\#}_{DYN}(P,T,\omega) \stackrel{\Delta}{=} \left(\Gamma^{\#}(P,T,\omega) - \Gamma^{\#}_{STAT}(P,T,\omega)\right) \quad (15)$$

Figure 1 shows a typical example of RPN, nRPN, $nRPN_{STAT}$, and $nRPN_{DYN}$ plots. The larger the difference between nRPN and RPN plots, the more nonlinear the system.

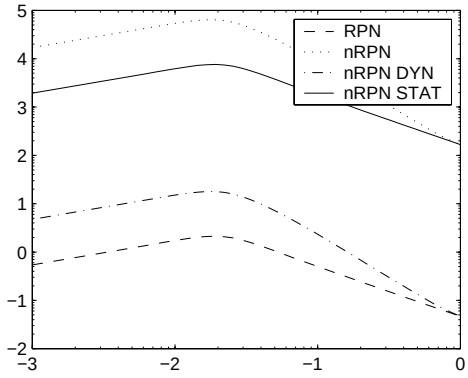

Fig. 1: RPN and nRPN curves for systems with static and dynamic of nonlinearity Note that the frequency is on a logarithmic scale so that -4 should be understood as 10^{-4}.

If the nonlinearity is purely static the difference between the nRPN and the RPN curves is constant for all frequencies, since the process models differ in the process gain only. Figure 2 illustrates this situation, which typically occurs for pH-reactors.

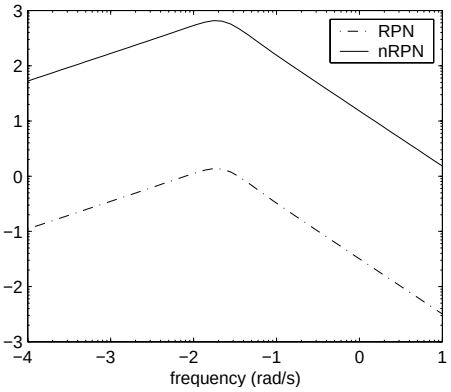

Fig. 2: RPN and nRPN curves for systems with pure static nonlinearity

Therefore, the nonlinearity can be parceled out into its static and dynamic component by adding to the RPN curve the minimum difference between the nRPN and RPN curves. This value corresponds to the nonlinear *static* RPN curve, as defined by (14). The dynamic component is given by subtracting from the total nonlinearity (nRPN curve) the static component ($nRPN_{STAT}$ curve) as in equation (15).

The analysis of the nRPN, $nRPN_{STAT}$, and $nRPN_{DYN}$ curves allow not only determining if a nonlinear controller is necessary, but also allows choosing the characteristics of the nonlinear controller that would be necessary for a given plant, what is very important for several practical applications. For example, if the $nRPN_{DYN}$ and RPN curves are closer to each other and the difference between $nRPN_{STAT}$ and RPN curves is large, a nonlinear controller with simple static gain compensation (gain scheduling controller) is recommended to improve the control performance. In this case, a controller with variable dynamic will not produce a better result. It is important to mention that nonlinear controllers with fix dynamic are much simpler to develop and maintain.

3.3 Nonlinear RPN indices

In the last section, it was shown that analyzing the nRPN curves is possible to quantify the process nonlinearities. For practical and quick analysis it is better to quantify the process nonlinearities using numbers (indices) instead of graphics. Therefore, to capture the distance between the nRPN curves we will introduce the nRPN, $nRPN_{STAT}$, and $nRPN_{DYN}$ indices. These indices are defined by the relative difference between the areas under the curves, i.e.,

$$\begin{aligned} nRPN &\stackrel{\Delta}{=} \log_{10}\left(\frac{A_{nRPN} - A_{RPN}}{A_{RPN}}\right) \\ nRPN_{STAT} &\stackrel{\Delta}{=} \log_{10}\left(\frac{A_{nRPN\_STAT} - A_{RPN}}{A_{RPN}}\right) \\ nRPN_{DYN} &\stackrel{\Delta}{=} \log_{10}\left(\frac{A_{nRPN\_DYN} - A_{RPN}}{A_{RPN}}\right) \end{aligned} \quad (16)$$

The areas are defined as follows:

$$\begin{aligned} A_{RPN} &\stackrel{\Delta}{=} \int_{\omega_{\min}}^{\omega_{\max}} \Gamma(G,T,\omega)\, d\log\omega \\ A_{nRPN} &\stackrel{\Delta}{=} \int_{\omega_{\min}}^{\omega_{\max}} \Gamma^{\#}(P,T,\omega) d\log\omega \\ A_{nRPN\_STAT} &\stackrel{\Delta}{=} \int_{\omega_{\min}}^{\omega_{\max}} \Gamma^{\#}_{STAT}(P,T,\omega) d\log\omega \\ A_{nRPN\_DYN} &\stackrel{\Delta}{=} \int_{\omega_{\min}}^{\omega_{\max}} \Gamma^{\#}_{DYN}(P,T,\omega) d\log\omega \end{aligned} \quad (17)$$

It was introduced the logarithm function in the definition of nonlinear indices to make easier their interpretation. Values smaller than 1 indicate that the performance difference between nonlinear and linear controllers is not significant, so that a linear controller is recommended. Indices greater than 2 clearly indicate that a nonlinear controller is necessary. Between 1 and 2 is a transition zone, where in many times a robust controller can stabilize all possible plants, but the performance loss can be significant.

4 CASE STUDY: HIGH PURITY DISTILLATION COLUMN

Distillation columns are currently the main separation process applied in chemical and petrochemical industries (Luyben, 1992). The control of high purity distillation columns generally is not an easy task, due to the coupling between the controlled variables, susceptibility to the external unmeasured disturbances and often high non-linearity degree. Small disturbances in high purity columns are responsible for great change in the product compositions. Moreover, these columns shows high time constants and asymmetric gain variation.

In this section the nonlinearity degree of an industrial high purity distillation column used to split Benzene from Toluene from a misture Benzene-Toluene-Xilenes (BTX).

4.1 Process Description

The distillation column operates at atmospheric pressure, being fed with a mixture of BTX and small quantity of water. The column has 40 theoretical trays. The benzene is removed in a sidestream withdraw laterally at the third theoretical tray from the top. At the top, due to a subcooling the small quantity of water is separate from benzene in a two phase drum. Fig.3 shows schematically the distillation column.

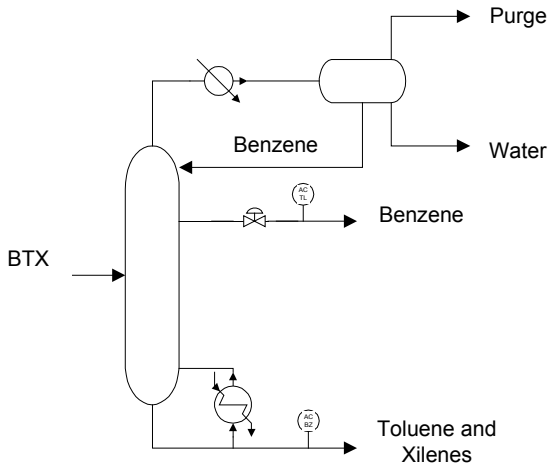

Fig. 3: Schematic representation of the Benzene column of a typical BTX unit

The controlled variables are benzene contamination in the bottom stream and toluene concentration in the sidestream. To control the compositions the corresponding manipulated variables are reboiler heat duty and sidestream flowrate.

A rigorous dynamic model of the benzene column was built in the commercial simulator Aspen Dynamics 11.1 using NRTL thermodynamic model for the liquid phase. This dynamic model can satisfactory describe the actually behavior of the real column.

4.2 Operating Regions

The operating space is divided in six operating regions defined by different compositions expressed in ppm of benzene in the bottom stream and toluene in the siedestream. Table 1 shows the operating regions analyzed in this paper. For example, the OR1 of Table 1 means that the composition of benzene and toluene are 50 ppm in the bottom and siede streams, respectively. The OR1 to OR4 are high purity operating points meaning high non-linearity degree, whilst OR5 and OR6 can be considered as moderate purity operating points.

Table 1: Definition of the Operating Regions (OR)

	Toluene (ppm) in the Siedestream		
Benzene (ppm) in the Bottom Stream		**50**	**200**
	50	OR1	OR2
	200	OR3	OR4
	100	OR5	OR6

Figures 4 and 5 respectively show the static gain and settling time for the transfer function of the channel (toluene impurity)/(siedestream flowrate). The transfer functions were obtained for several toluene composition in the siedestream with a fix benzene composition in the bottom stream equal to 50 ppm. Note that both gain and settling time abruptly change when the toluene composition is lower than 200 ppm. The gain and settling time change approx. 100 and 40 times, respectively.

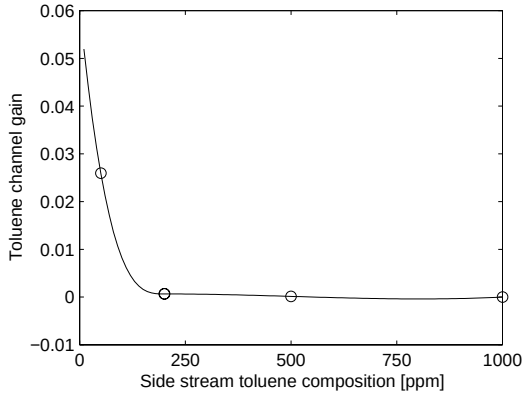

Fig. 4: Curve of the static gain for several specifications of toluene impurity with a 50 ppm benzene loss in the bottom stream.

Table 2 and 3 respectively show the gain matrix and settling time of the linearized models. These Tables indicates that the behavior presented in Figures 4 and 5 can be extended to the other channels.

The qualitative analysis of the non-linearity degree indicates that the regions of high purity (OR1 to OR4) exhibit a great variation in the static gain and dynamics. However, the regions where the specifications are moderated (OR5 and OR6), the non-linearity is less pronounced.

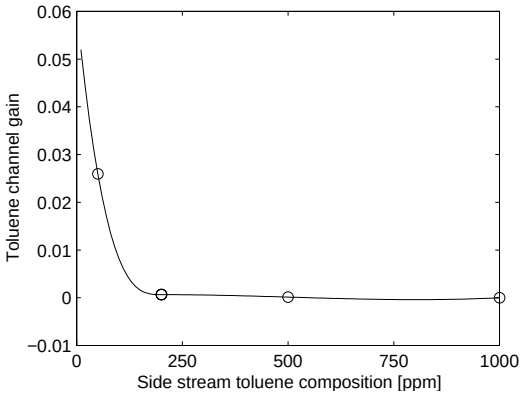

Fig. 5: Settling time for several specifications of toluene impurity and fix 50 ppm benzene loss in the bottom stream.

Table 2: Gain Matrix for the OR defined in Table 1. The output are toluene impurity and benzene loss (rows) and the manipulated variables are Sidestream flowrate and heaty duty (columns)

	50	200
50	$\begin{bmatrix} 0{,}026 & 0{,}16 \\ -0{,}13 & -0{,}86 \end{bmatrix}$	$\begin{bmatrix} 0{,}051 & 0{,}33 \\ -0{,}041 & -0{,}27 \end{bmatrix}$
200	$\begin{bmatrix} 0{,}007 & 0{,}0043 \\ -0{,}056 & -0{,}37 \end{bmatrix}$	$\begin{bmatrix} 0{,}0044 & 0{,}029 \\ -0{,}051 & -0{,}34 \end{bmatrix}$
1000	$\begin{bmatrix} 0{,}0002 & 0{,}0014 \\ -0{,}052 & -0{,}34 \end{bmatrix}$	$\begin{bmatrix} 0{,}0002 & 0{,}0014 \\ -0{,}052 & -0{,}34 \end{bmatrix}$

Table 3: Settling time (min)

	50	200
50	1900	500
200	200	100
1000	45	45

4.3 nRPN Analysis

Fig. 6 shows the nRPN curves for each OR calculated using a desired performance of 10 min rise time and 5% overshoot. The set of linear models used in each region was: the linear model determined in the nominal operating point and the models with the composition twice greater in each component (e.g. the OR1, was described by the linear models with (1) 50 and 50 ppm, (2) 100 ppm and 50 ppm, and (3) 50 ppm and 100 ppm of toluene impurity and benzene loss). Table 4 summarizes the corresponding values of the nRPN, $nRPN_{DYN}$ and $nRPN_{STAT}$ indixes.

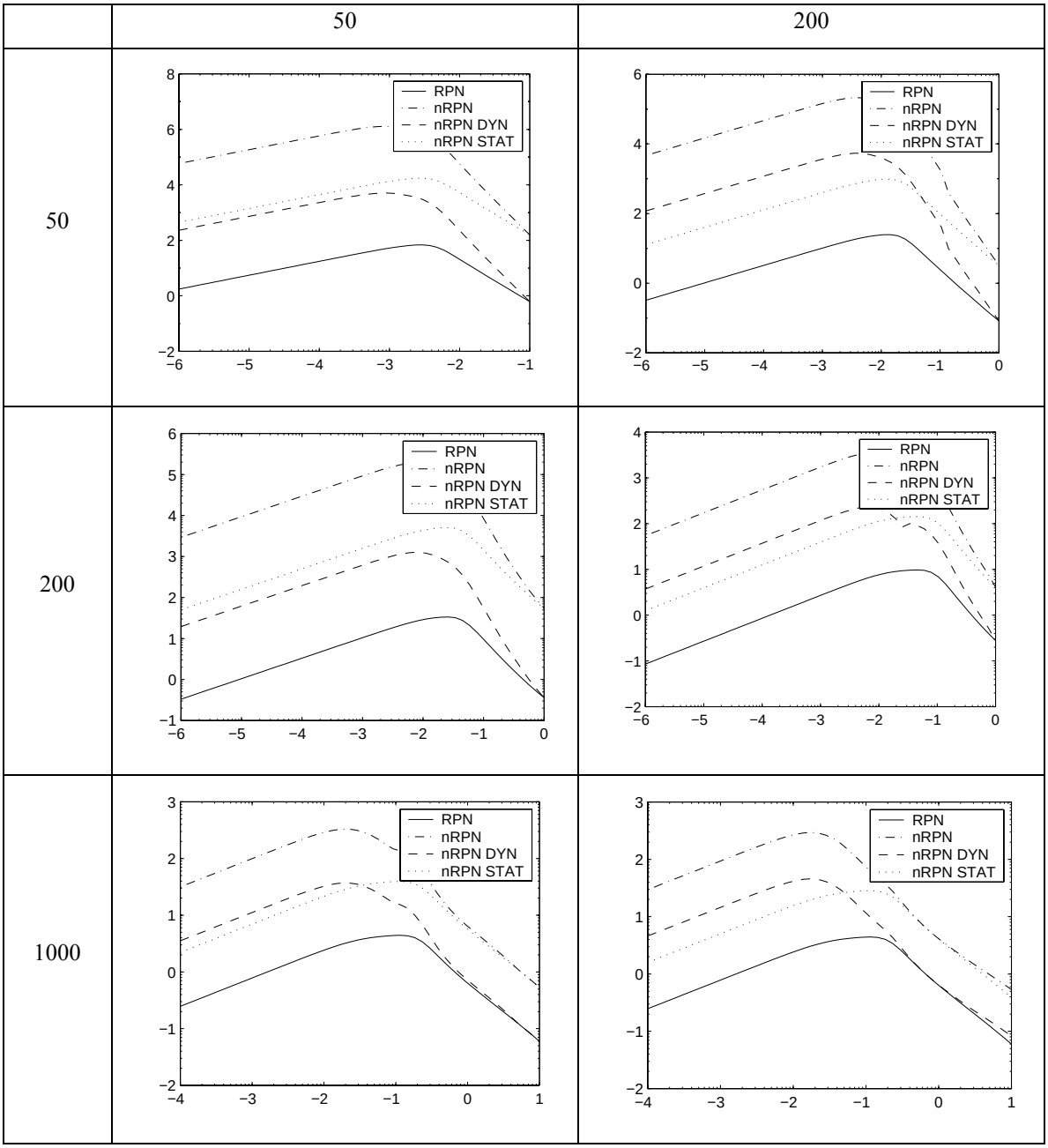

Fig.6: nRPN curves for each operating regions

Table 4: nRPN indexes corresponding to Fig. 6

	nRPN	$nRPN_{DYN}$	$nRPN_{STAT}$
OR1	3,85	1,43	2,40
OR2	3,49	1,89	1,58
OR3	3,31	1,10	2,18
OR4	1,99	0,75	1,13
OR5	1,24	0,04	0,90
OR6	1,05	-0,05	0,74

Analyzing Fig. 6 and Table 4, we can conclude that the OR1 to OR3 are the most nonlinear exhibiting both static and dynamic nonlinearities. To control the column at these regions it is necessary to apply a controller which can compensate both static and dynamic behavior. For OR4, the plant can be already controlled by a nonlinear controller with static compensation only (e.g., gain schedule controller). In this region the dynamic nonlinearity is not too pronounced. The OR5 and OR6 can be controlled by linear controllers. If tight performance is required for these OR, a simple static compensation will do the job quite well.

To show the effect of velocity of the closed loop in the nonlinear degree, the column operating at OR5 was simulated with 3 controllers with the following relations between the closed loop and open loop dynamic: (a) twice faster, (b) 6 times faster, and (c) 12 times faster. The simulations results with decentralized PI controllers which achieve these

relations are show in Fig. 7 for disturbances with different magnitudes. The responses were normalized by the disturbance magnitude to make easier the analysis. Fig. 7 clearly shows that the faster the controller (closed loop), less nonlinearity degree exhibit by the plant. Note that the effect of closed loop velocity is captured automatically in the nRPN, as can be seen in Table 5. Note that for faster closed loop response the nRPN is smaller indicating a smaller nonlinearity degree.

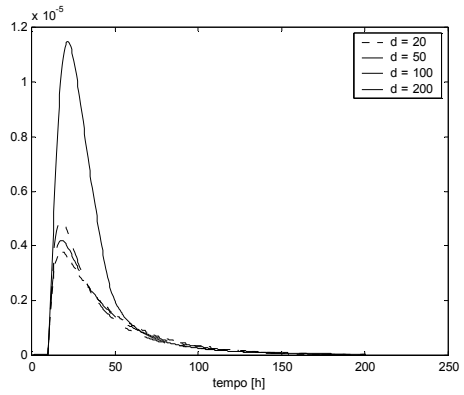

(a)

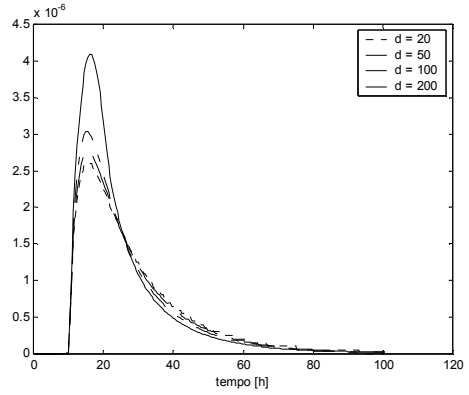

(b)

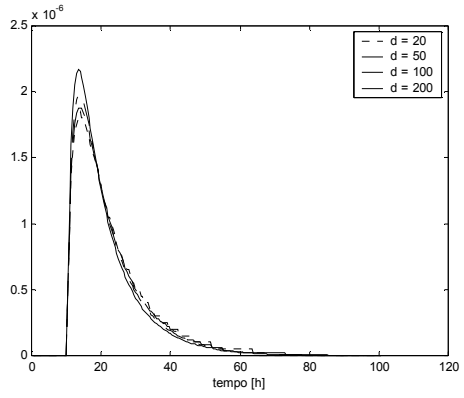

(c)

Fig.7: Simulation in closed loop with decentralized PI controllers for OR5 and different relations between the closed loop and open loop dynamic: (a) twice faster, (b) 6 times faster, and (c) 12 times faster.

Table 5: nRPN for OR5 and several rise time for the closed loop response

Rise Time [min]	nRPN
1	0.96
10	1.24
20	1.38
50	1.58
100	1.70
200	1.79

5 QUADRUPLE-TANK PLANT

5.1 Process description

The quadruple-tank process (see Fig. 8) is a laboratory process that consists of four interconnected water tanks. The linearized dynamic model of the system has a real multivariable zero, whose sign can be changed depending on operating conditions. In this way, the quadruple-tank process is ideal for illustrating many concepts in multivariable control, particularly performance limitations due to multivariable RHP zeros. The location and the direction of zero have an appealing physical interpretation. The target is to control the level in the lower two tanks (i.e., h_1 and h_2) with the inlet flowrates, F_1 and F_2.

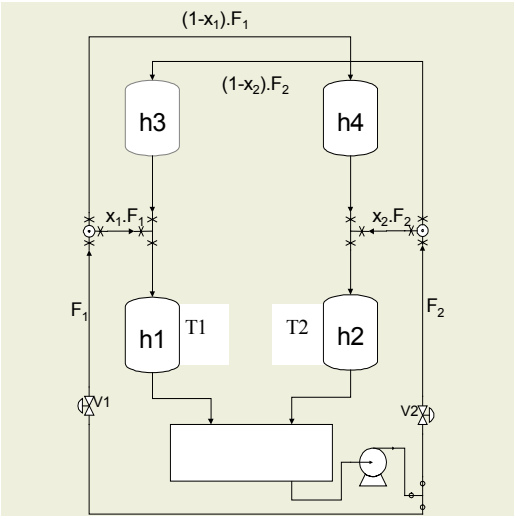

Fig. 8: Schematic representation of the quadruple-tank system

5.2 Process Model

The process model consists of the mass balance around each tank and is given by

$$\begin{aligned} A_1 \frac{dh_1}{dt} &= x_1 \cdot F_1 + R_3\sqrt{h_3} - R_1\sqrt{h_1} \\ A_2 \frac{dh_2}{dt} &= x_2 \cdot F_2 + R_4\sqrt{h_4} - R_2\sqrt{h_2} \\ A_3 \frac{dh_3}{dt} &= (1 - x_2) \cdot F_2 - R_3\sqrt{h_3} \\ A_4 \frac{dh_4}{dt} &= (1 - x_1) \cdot F_1 - R_4\sqrt{h_4} \end{aligned} \tag{18}$$

where A_i is the cross-section area of Tank i, R_i is the outlet flow coefficient of Tank i, h_i is the water level of Tank i, F_1 and F_2 are the manipulated inlet flowrates and x_1 and x_2 are the valve distribution flow factors $0 \le x_i \le 1$.

The parameters used in this work are basically the same as those in (Johansson, 2000) and are given by $A_1 = A_3 = 28$ cm^2, $A_2 = A_4 = 32$ cm^2, $R_1 = R_3 = 3.145$ cm$^{2.5}$/s and $R_2 = R_4 = 2.525$ cm$^{2.5}$/s.

5.3 Operating Points

The quadruple-tank process is studied at a minimum-phase operating point (MOP) and at a nonminimum-phase operating point (NMOP), due to the presence of the RHP transmission zero. Table 6 summarizes the operating conditions of MOP and NMOP. Note that the main difference between the OPs is the valve distribution flow factors, x_1 and x_2, which are responsible for the difference in h_3 and h_4 levels. All other variables are almost the same for both OPs.

Table 6: Definition of the Operating Points

Variables	MOP	NMOP
h_1, h_2 [cm]	12.26, 12.78	12.44, 13.16
h_3, h_4 [cm]	1.63, 1.41	4.73, 4.99
F_1, F_2 [cm^3/s]	9.99 , 10.05	9.89, 10.36
x_1, x_2 [-]	0.7, 0.6	0.43, 0.34

Table 7: RHP zero and RGA

	MOP	NMOP
RHP zero	none	0.0128
RHP zero input direction	_	$u_z = \begin{bmatrix} 0.7326 \\ -0.6806 \end{bmatrix}$
RHP zero output direction	_	$yz = \begin{bmatrix} -0.7743 \\ 0.6329 \end{bmatrix}$
RGA(0)	$\begin{bmatrix} 1.4 & -0.4 \\ -0.4 & 1.4 \end{bmatrix}$	$\begin{bmatrix} -0.64 & 1.64 \\ 1.64 & -0.64 \end{bmatrix}$

5.4 RHP Zero and RGA

Johansson (2000) shows that the quadruple-tank system always has two transmission zeros, whose locations can be classified based on the $x_1 + x_2$ value. When $0 < x_1 + x_2 < 1$, one of the transmission zeros is located in RHP. For the case where $x_1 + x_2 = 1$, the system has a transmission zero at the origin, whereas for $1 < x_1 + x_2 < 2$ no RHP zero occurs. Table 7 shows the RHP zeros for both OPs. For NMOP, the input zero direction, u_Z, and output zero direction, y_Z, were also included in the table. The steady-state RGA (see Table 7) clearly shows that the pairing used for MOP (i.e., (F_1, h_1) and (F_2, h_2)) should not be applied to NMOP. When the system operates in NMOP the pairing is inverse, due to the transmission zero that changes its signal. A complete analysis about the controllability to the quadruple-tanks system is presented in Trierweiler and Farina (2002)

5.5 Analysis of the Nonlinearity Degree

To calculate the nonlinearity degree it is necessary to define a set of possible plants. Here, we will analyze the degree of nonlinearity against to inlet flow variation (i.e., F_1 and F_2) and to split ratio variation (i.e., x_1 and x_2).

Table 8: Inlet flowrates used for linearizing the nonlinear model

	Model 1	Model 2	Model 3
F_1 [cm^3/s]	8	12	10
F_2 [cm^3/s]	12	8	10

5.6 Influence of inlet flows F_1 and F_2

The set of models used in the analysis of inlet flow influence is defined in Table 8. The polytopic model used in the analysis is obtained by linearizing the nonlinear model at the steady state conditions corresponding to F_1 and F_2 as shown in Table 8 and for x_1=0.7 and x_2=0.6 in the case of MOP and x_1=0.43 and x_2=0.34 for NMOP.

Results for MOP

The analysis of nRPN and RPN curves indicates that the system is practically linear for inlet flowrate variations, as we can see in Fig. 9. This figure was obtained using a desired performance of 50 sec rise time and 5% overshoot.

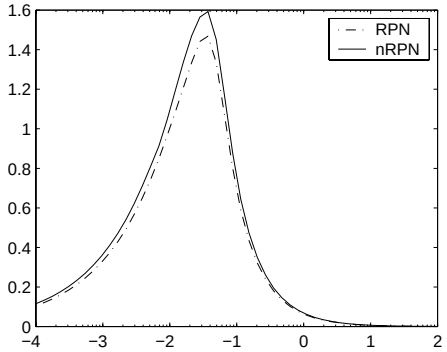

Fig. 9: nRPN and RPN plots for MOP and inlet flow variations.

Table 9 shows the corresponding nRPN indices for the influence of the feed flowrate. Note that the nonlinearity is very small and it is almost static, since

nRPN ≈ $nRPN_{STAT}$. The dynamic nonlinearity is almost non-existent (i.e., $nRPN_{DYN}$= -1.84).

Table 9: nRPN indices for MOP and inlet flowrate variations

nRPN	$nRPN_{STAT}$	$NRPN_{DYN}$
-1.33	-1.84	-1.49

Fig. 10a shows the closed loop response of the nonlinear dynamic model for different setpoint changes in h_1. Two decentralized linear PI controllers were used in the simulation. In Fig. 10b the responses are normalized by the step change. This figure clearly confirms that the system is practically linear.

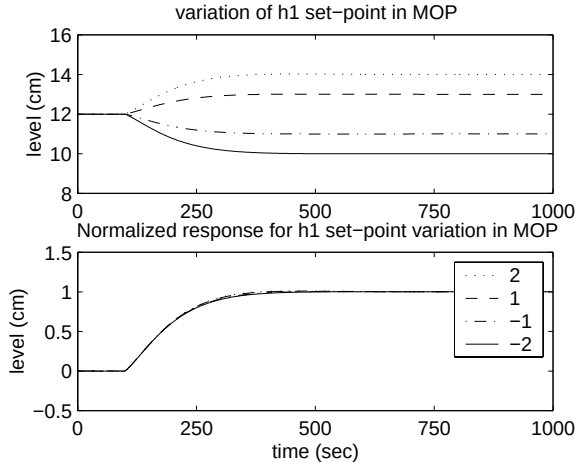

Figure 10: Closed loop step response several setpoint changes

Results for NMOP

Very similar results are obtained for the NMOP (not shown here). Therefore, we can conclude that the system is weak nonlinear against inlet flowrate variation. Simple linear controllers will succeed to control the system at least for the inlet flows listed in Table 8.

Influence of the distribution ratios x_1 and x_2

In this section, the influence of x1 and x2 in the degree of nonlinearity will be measured. x1 and x2 are responsible for the location of the transmission zeros, what can increase the nonlinearity degree.

Table 10: Distribution Ratio used to construct the polytopic model for MOP

	Model 1	Model 2
x_1 [-]	0.7	0.5
x_2 [-]	0.5	0.7

Results for MOP

The first operating region to be analyzed is around the minimum phase operating point (MOP). Table 10 shows the linear models that compose the polytopic model.

Fig. 11 shows the nRPN and RPN plots for the MOP. The desired performance was 50-sec rise time and the 5% overshoot. Table 11 presents the nRPN indices for the influence of the feed distribution ratio. Based on these results, it can be concluded that the system is weak nonlinear and a linear controller performs well.

Table 11: nRPN indices for x1 and x2 variations and MOP

NRPN	$nRPN_{STAT}$	$nRPN_{DYN}$
-0.024	-0.040	-1.73

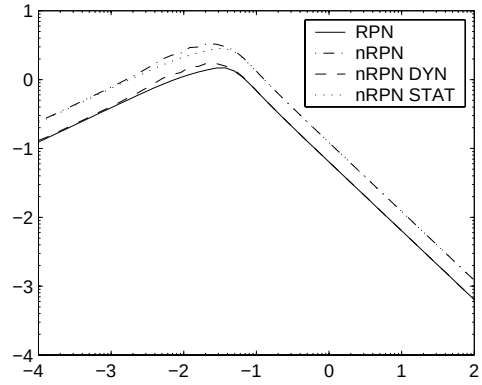

Fig. 11: nRPN and RPN plots for x1 and x2 variations and MOP (both axes are in logarithmic scale).

Fig.12 shows the closed loop response of the nonlinear dynamic model for the operating points defined by (x1,x2) = (0.8,0.7), (0.7,0.6), and (0.6, 0.7).

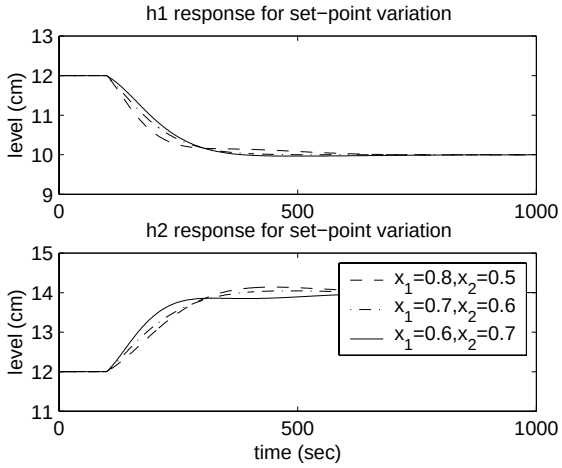

Figure 12: Closed loop step response for MOP and (x1,x2) = (0.8,0.5), (0.7,0.6), and (0.6, 0.7)

For each one of these operating points, the setpoint h1 and h2 were simultaneouly changed by -2 and 2 units, respect. A full linear PI controller was used in the simulation. This figure clearly confirms that a simple linear controller will perform well.

Results for NMOP

For the NMOP the set of models that will be analyzed is defined in Table 12. This OR shows a transmission zero located in RHP, causing inversion in the determinant of the gain matrix. The right pairing for NMOR is (F1-h2) and (F2-h1).

Table 12: Distribution Ratio used to construct the polytopic model for NMOP

	Model 1	Model 2	Model 3
x_1 [-]	0.5	0.3	0.2
x_2 [-]	0.3	0.5	0.2
RHP zero	0.0119	0.0111	0.0498

Figure 13 shows the nRPN and RPN plots for NMOR. This figure was obtained using a desired performance of 50 sec rise time and 5% overshoot. Table 13 shows the nRPN indices for the influence of the feed distribution ratio. Based on these results, it can be concluded that the NMOP is more nonlinear than the MOP, but a linear controller still performs well. nRPN lower than 1 indicates that a linear controller will perform satisfactory. Above this value, the benefits of a nonlinear controller become more evident.

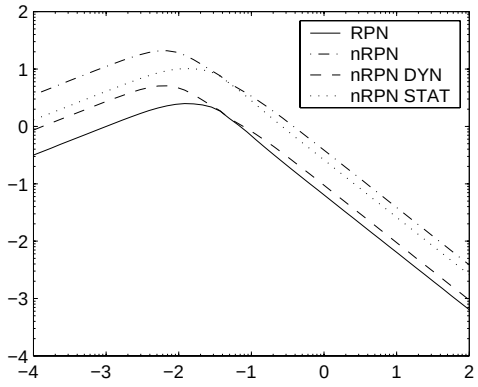

Figure 13: nRPN and RPN plots for x1 and x2 variations and NMOP (both axes are in logarithmic scale).

Table 13: nRPN indices for x1 and x2 variations and NMOR

nRPN	$nRPN_{STAT}$	$nRPN_{DYN}$
0.680	0.490	-0.380

Figure 14 shows the closed loop response of the nonlinear dynamic model for the operating points defined by (x1,x2) = (0.2,0.2), (0.5,0.3), and (0.35, 0.25). For each one of these operating points, the setpoint h1 and h2 were simultaneously changed by -2 and 2 units, respect. A full linear PI controller was used in the simulation. This figure clearly confirms that a simple linear controller will perform well. Note that for the NMOP there is a little performance degradation if compared to the MOP. If it is decided to applied a nonlinear controller, a simple gain scheduling controller is recommended, since the nonlinearity is mainly static (see Table 13).

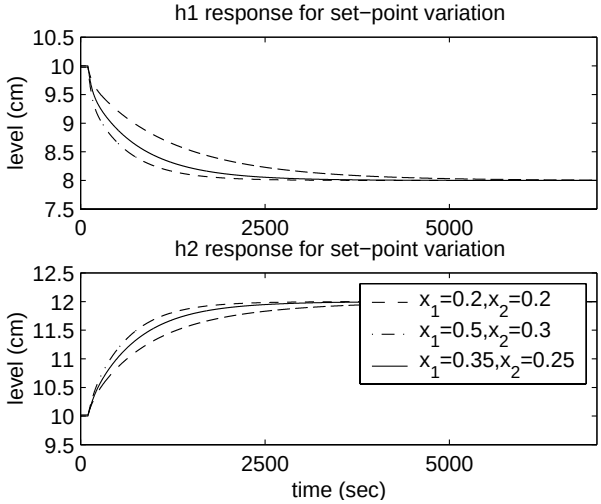

Figure 14: Closed loop step response for MOP and (x1,x2) = (0.2,0.2), (0.5,0.3), and (0.35, 0.25).

Results for both MOP and NMOP

Now, it is analyzed the case where both operating region are included. The linear models used to calculate the degree of nonlinearity are listed in Tables 10 and 12.

Figure 15 shows the nRPN and RPN plots for NMOR/MOR. This figure was obtained using a desired performance of 50-sec rise time and 5% overshoot.

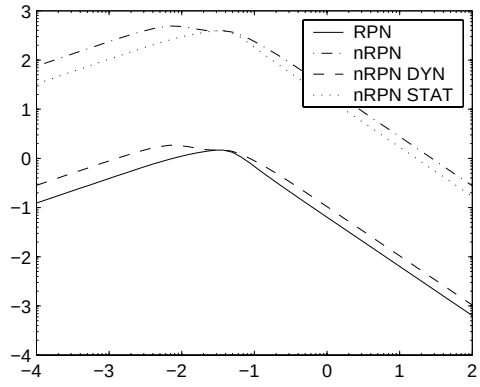

Figure 15: nRPN and RPN plots for x1 and x2 variations and NMOP/MOP (both axes are in logarithmic scale).

Table 14 shows the corresponding nRPN indices. Based on these results, it can be concluded that the NMOR/MOR is much more nonlinear than the MOR and NMOR separately. The reason is that the multivariable process gain changes its sign, so that a nonlinear controller is required.

Table 14: nRPN indices for x1 and x2 variations and NMOP/MOP

nRPN	$nRPN_{STAT}$	$nRPN_{DYN}$
2.60	2.42	-0.285

Figure 16 shows the simulation results produced by a nonlinear model predictive controller (Duraisk, 2001). With this kind of controller it is possible to work with the system in both operating regions. Equivalent simulations with linear controllers are unstable.

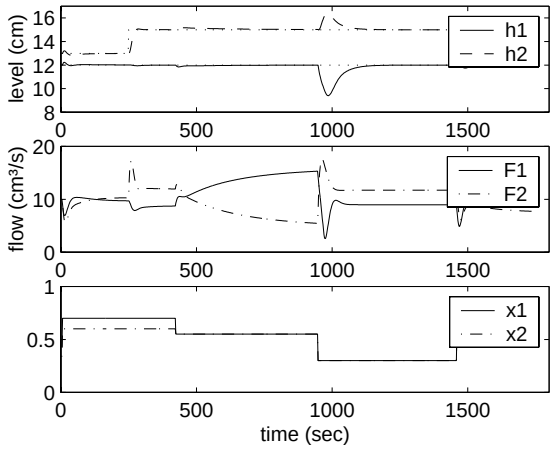

Figure 16: Set-point change and disturbance rejection capability for NMOP/MOP using NMPC (a) controlled variables and (b) manipulated variables and (c) disturbances.

The main reason for the high nonlinearity is the sign inversion of the gain matrix. If we invert the pairing for only the NMOP models, the total nonlinearity must decrease, because the inversion disappears. Figure 17 shows the nRPN and RPN plots for NMOR/MOR, where the models corresponding of NMOP have been modified to fit the (F1-h2) and (F2-h1) pairing. Table 15 shows the corresponding nRPN indices. Based on these results, we can concluded that a linear controller can stabilize the control loop if a switching mechanisms is implemented to select the correct pairing based on the operating region.

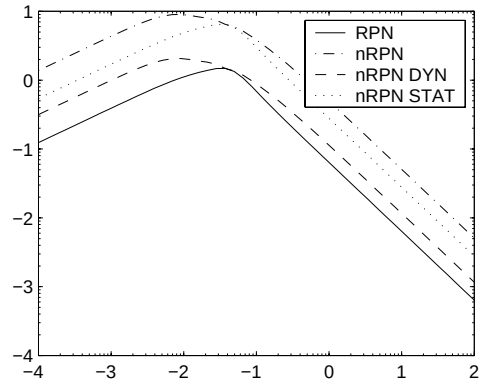

Figure 17: nRPN and RPN plots for x1 and x2 variations and NMOP/MOP (both axes are in logarithmic scale).

Table 15: nRPN indices for x1 and x2 variations and NMOP/MOP changing the paring of NMOP

$nRPN_R$	$nRPN_{STAT}$	$NRPN_{DYN}$
0.79	0.53	-0.19

6 CONCLUSIONS

Three novel indexes were introduced to measure system's nonlinearity. These nonlinear measurements are derived from the Robust Performance Number (RPN) concept. The total system's nonlinearity can be measured by the *nonlinear RPN* (nRPN), while the purely static nonlinearity is captured by nonlinear static RPN ($nRPN_{STAT}$) and the dynamic component by the nonlinear dynamic RPN ($nRPN_{DYN}$). The novel indexes do not require a nonlinear model, being enough a set of linear models. Therefore, they can easily be applied to quantify the nonlinearities of industrial plants and used to answer several practical important questions such as: how nonlinear is the system? Is it necessary to apply a nonlinear controller? What kind of nonlinear controller is necessary?

The novel indices were applied to quantify the nonlinearity degree of two case studies: an industrial high purity distillation column and the quadruple-tanks system. For the quadruple-tanks system the nonlinearity was quantified against inlet flow and distribution ratio variations. This system can perform well in almost all situations. The only condition that requires a nonlinear controller is the case where the system goes from the NMOP to MOP and vice-versa. The predictions made by nRPN indices were confirmed by nonlinear simulations with linear controllers.

ACKNOWLEDGMENT

The authors thank PETROBRAS/BRASKEM/ FINEP for supporting this work.

REFERENCES

Duraisk, R. G. (2001); Controlador Preditivo Não-Linear Utilizando Linearizações ao Longo da Tragetória; *Dissertação de Mestrado.UFRGS.*

Guay, M., McLellan, P., Bacon, D. W. (1997). Measure of Closed-Loop Nonlinearity and Interaction for Nonlinear Chemical Processes. *AiChe Journal*. Vol: 43 (9), 2261-2278.

Helbig, A., Marquardt W., Allgöwer F. (2000). Nonlinearity Measures: Definition, Computation, *Applications. Journal of Process Control* 10: 113-123.

Johansson, K. H.; The Quadruple Tank Process: A Multivariable Laboratory with a Adjustable Zero; *IEEE Transactions on Control Systems Tecnology*; Vol. 8, Nº3, May 2000

Klatt, K., Engell, S (1996); Nonliner Control of Neutralization Processes by Gain-Scheduling Trajectory Control, *Ind. Eng. Chem. Res.*, 35, pp 3511-3518.

Luyben, W., L. (1992); *Practical Distillation Control*; Van Nostrand Reinhold.

Skogestad, S. and I. Postlethwaite (1996). Multivariable Feedback Control _Analysis & Design. John Wiley&Sons.

Trierweiler, J.O. and S. Engell (1997a). The Robust Performance Number: A New Tool for Control Structure Design. *Comp. chem. Eng.,* (21), *Suppl.,* pp. S409-414.

Trierweiler, J.O. (1997). A Systematic Approach to Control Structure Design. *Ph.D. Thesis,* Univ. of Dortmund.

Trierweiler, J. O. , Farina, L.A. (2002). The RPN Metodology Apllied to Quantify Process Operability and Control Design *IFAC-World Congress*.